BMC Infectious Diseases

RESEARCH

Open Access

Revealing the progression and pathologic features of intraperitoneal infection of *Trichomonas vaginalis* in mice via parasite α-actinin-based immunological detection

Yiting Xie[1,2], Congxi Zhang[1], Petrus Tang[3], Geoff Hide[4], Dehua Lai[1*] and Zhao-Rong Lun[1,4*]

Abstract

Background Trichomoniasis caused by *Trichomonas vaginalis* is the most prevalent nonviral sexually transmitted disease in women and has frequently damaged public health. To better use the animal model and take a step forward fully elucidating this pathogen, intraperitoneal infection of *T. vaginalis* in mice, one of the most common mouse models, was highly concerned.

Methods By adjusting the number of parasites inoculated, acute and chronic infection models were established. Pathological changes and the presence of *T. vaginalis* in organs were observed at different timepoints post inoculation using histological and TV-α-actinin-based immunological detection.

Results The results reconfirmed the correlation between inoculum size of parasites and infection duration, as well as the multiplication capacity of *T. vaginalis* in mouse enterocoelia or invaded organs. The progression and pathologic features of vital organs (e.g., liver and spleen) from mice intraperitoneally infected with *T. vaginalis* in both the acute and chronic groups were also revealed. In particular, a reliable immunological method based on TV-α-actinin was first verified to clearly present the invasion of *T. vaginalis* into infected mouse organs.

Conclusions In brief, this study presented a clearer and more detailed pathologic characteristic of the intraperitoneal infection model, which probably provides more basic information for the use of this model in future studies. Especially, expanding on specific research applications of this model would be valuable.

Keywords *Trichomonas vaginalis*, TV-α-actinin, Intraperitoneal infection model, Pathogenesis, Immunodetection

*Correspondence:
Dehua Lai
laidehua@mail.sysu.edu.cn
Zhao-Rong Lun
lsslzr@mail.sysu.edu.cn
[1]MOE Key Laboratory of Gene Function and Regulation, State Key Laboratory of Biocontrol, School of Life Sciences, Sun Yat-Sen University, Guangzhou 510275, China
[2]Department of Human Parasitology, School of Basic Medical Science, Hubei University of Medicine, Shiyan 442000, China
[3]Bioinformatics Core Laboratory, Chang Gung University, Taoyuan 333, Taiwan
[4]Biomedical Research Centre and Ecosystems and Environment Research Centre, School of Science Engineering and Environment, University of Salford, Salford M5 4WT, UK

© The Author(s) 2024. **Open Access** This article is licensed under a Creative Commons Attribution-NonCommercial-NoDerivatives 4.0 International License, which permits any non-commercial use, sharing, distribution and reproduction in any medium or format, as long as you give appropriate credit to the original author(s) and the source, provide a link to the Creative Commons licence, and indicate if you modified the licensed material. You do not have permission under this licence to share adapted material derived from this article or parts of it. The images or other third party material in this article are included in the article's Creative Commons licence, unless indicated otherwise in a credit line to the material. If material is not included in the article's Creative Commons licence and your intended use is not permitted by statutory regulation or exceeds the permitted use, you will need to obtain permission directly from the copyright holder. To view a copy of this licence, visit http://creativecommons.org/licenses/by-nc-nd/4.0/.

Background

Trichomonas vaginalis (TV) is the etiological agent of human trichomoniasis, which affects approximately 156.3 million people worldwide [1]. In addition to the commonly reported inflammation of the urogenital system in symptomatic patients, many secondary effects, such as an increasing risk of infection associated with human immunodeficiency virus (HIV) [2], prostate cancer [3, 4] and adverse outcomes of pregnancy [5, 6], have been frequently reported.

Although great progress has been made in research on *T. vaginalis* thanks to the efforts of scientists worldwide, trichomoniasis caused by this parasite is still referred to as a neglected sexually transmitted disease [7]. This, in our opinion, is partially attributed to the difficulty in validation of many extraneous research findings about *T. vaginalis* or directly conducting related studies in vivo due to the lack of perfect experimental animal models. Therefore, animal models, especially commonly used mouse models, need further study. There are three common mouse models of this parasite: the vaginal model, subcutaneous model and intraperitoneal model. They have their own advantages and weaknesses and have made important contributions to studies of *T. vaginalis*. However, considering the complexity of vaginal modeling in mice, the difficulty in maintaining a high infection rate for a long time and the possibility of an immune response affected by estrogen treatment in a vaginal model [8–10], as well as the limited correlation between local abscess and clinical manifestations in a subcutaneous model [11], our laboratory paid much attention to the further study of the intraperitoneal model that usually presents a stable infection rate and prominent pathological changes.

As one of the most common animal models, peritoneal infection of *T. vaginalis* in mice has been widely used for studies, such as vaccine evaluation [12–14], drug screening [15–18], virulence assessment of isolates, metronidazole susceptibility assays [19–21], revealing the interplay between immune cells and parasites [22] and even the immune evasion strategy [23]. In earlier studies, *T. vaginalis* infection has been shown to cause a range of clinical symptoms, multiorgan disease and death in mice, and histopathology studies with hematoxylin and eosin (H&E) staining also revealed pathological features in the viscera of mice [10, 24, 25]. However, in previous studies from our laboratory, it was found that using the same isolate of *T. vaginalis* could establish acute and chronic models by adjusting the parasite number and observation period. But, their differences in progression and pathologic manifestations have seldom been reported. Additionally, trichomonas in pathological sections were often difficult to be identified, especially after the parasites invading into tissues/organs and experiencing the amoeba-like deformation [26], making it a great challenge to identify the distribution of *T. vaginalis* in different organs from the infected mice at different stages. Therefore, if *T. vaginalis* could be clearly displayed in infected organs, for example, by targeting a specific *T. vaginalis* antigen, a clearer understanding of the pathogenesis and pathological features will be obtained.

T. vaginalis alpha-actinin (TV-α-actinin), a type of actin-binding protein, is a virulence factor of the parasite derived from the cytoskeleton [27]. As a structural protein, it can be continuously expressed during the parasite life without geographical variation [27]. Of note, it has been identified as the most common immunogen from *T. vaginalis* recognized by sera from *T. vaginalis*- infected female patients [28, 29]. In addition, studies have shown that antibodies against TV-α-actinin did not cross-react with human α-actinin or with homologous proteins from parasites such as *Entamoeba histolytica*, *Acanthamoeba castellanii*, *Giardia lamblia*, and *Leishmania major* [27]. Therefore, TV-α-actinin, with high immunogenicity, high conservation and high specificity, can be used as an ideal target for trichomonal immunodiagnosis.

Briefly, this study, by using TV-α-actinin as an immunologically diagnostic target of *T. vaginalis*, revealed the more extensively characterized pathogenesis progression and pathologic features of both acute and chronic models of intraperitoneal infection with *T. vaginalis*. In particular, the whereabouts, distribution and amount of *T. vaginalis* are expected to provide a more detailed theoretical basis for the application of the peritoneal model.

Methods

Isolates of *T. vaginalis* and animals

In this study, the *T. vaginalis* (CPOTV21) strain was isolated from a symptomatic outpatient in the Second Affiliated Hospital of Guangzhou Medical University and was used in all experiments [30]. For cultivation of this parasite, Diamond's trypticase-yeast medium [31] supplemented with 10% heat-inactivated fetal bovine serum (Excell, China), 100 U/ml penicillin and 100 μg/ml streptomycin was used. The cultures were maintained in a sterile incubator at 37 °C and subcultured every two days. Only logarithmic-phase parasites were used in this work.

Female Swiss mice (approximately 6–8 weeks old) were purchased from The Experimental Animal Center of Sun Yat-Sen University (Guangzhou, China). All animals were maintained in appropriate living conditions (25 °C±3 °C) under a 12 h/12 h light/ dark cycle and were entitled to freely consume a standard diet and pure water daily. Mice were euthanized by CO_2 at indicated time points. Protocols for the use of animals were approved by the Institutional Review Board for Animal Care of Sun Yat-Sen University (#31472058 and 31720103918).

Establishment of acute and chronic infection

Cultures of *T. vaginalis* at the logarithmic phase were centrifuged at 1000 ×g for 10 min. Then, the pellets were washed and resuspended in sterile PBS. After quantification by microscopy using a hemocytometer, the final concentration of *T. vaginalis* was adjusted with PBS as designed. Each mouse was intraperitoneally inoculated with the desired number of parasites in a 0.5 ml volume.

For the establishment of acute and chronic infection, Swiss mice were divided into 5 groups and intraperitoneally inoculated with 1×10^7 ($n=35$), 1×10^6 ($n=8$), 1×10^5 ($n=8$), 1×10^4 ($n=8$) *T. vaginalis* or sterile PBS (control, $n=8$) per mouse. Of which, the survival rate of the 1×10^7 inoculation group was accumulated from four independent assays in the early studies and one experiment conducted synchronously with other groups. According to the onset and survival time, inoculation of 1×10^7 *T. vaginalis* per mouse was defined as the acute model, while inoculation of 1×10^6 was defined as the chronic model. The survival states of all mice were monitored daily.

Parasite loading in ascites and pathologic scores

In the following studies, all assays were performed with these two models using Swiss mice. Five infected mice were sacrificed at each time point, including 1, 3, and 5 dpi for the acute group and 1, 3, 7, 14, 21, and 30 dpi for the chronic group. First, each mouse was intraperitoneally injected with 2 ml precooled PBS buffer and carefully rubbed for 1 min. Peritoneal fluid was obtained for direct quantification of *T. vaginalis* using a hemocytometer. Then, pathological scores were acquired according to the criteria published in a previous study [25] with minor modifications by excluding mortality-related points. In brief, the volume of ascites (score: 0–6), the damage level of peritoneum (score: 0–10), spleen/pancreas/stomach (score: 0–12), and livers (visceral, score: 0–10; diaphragmatic side, score: 0–12) were rated to obtain a final overall gross score (full mark: 50). Finally, the livers and spleens were removed and weighed. To further explore the pathological process, the liver and spleen were chosen as representative organs due to their obvious macroscopic lesions.

Alpha-actinin-based immunodetection

To verify the specificity and applicability of anti-TV-α-actinin sera prepared in our laboratory for immunodetection [12], dot-blot and immunocytochemistry (ICC) assays were first performed. In the dot-blot assay, a total of 1×10^7 *T. vaginalis* at logarithmic phase (positive sample: +) and 1×10^8 splenocytes from healthy mice (negative sample: -) were used for the preparation of whole-cell antigens through repeated freeze-thawing. In brief, the PVDF membrane soaked in methanol was first balanced in the transfer buffer solution for 1 min and then placed on filter paper for slight drying. After pointing the above samples with 10 µl for each dot, the film was incubated in 3% H_2O_2 solution for 10 min at room temperature, washed with TTBS (9 g NaCl, 20 ml 1 M Tris-Cl with pH7.6 and 1 ml Tween20 in 1 L ddH_2O), and then enclosed in TTBS solution containing 5% skim milk at 4 °C overnight. The anti-TV-α-actinin sera, including three dilutions (1:5000, 1:20,000 and 1:100,000), were incubated with three individual PVDF membranes for one hour at room temperature. After washing for three times, sheep anti-rabbit IgG antibody (1:500) labeled with HRP was added and incubated for another hour at room temperature. Finally, a DAB kit was used for color development.

For the ICC assay, *T. vaginalis* at the logarithmic stage was adjusted to 5×10^6 /ml and 100 µl was added to each slide pretreated with poly-L-lysine. After incubation at room temperature for 20 min, the unattached *T. vaginalis* were removed. The remaining parasites were fixed with precooled methanol for 20 min, hydrated in PBS for 20 min and then incubated with anti-TV-α-actinin sera (50 µl) diluted at 1:1000 at 37 °C for one hour. After washing for three times, HRP-enhanced anti-rabbit IgG antibody (ZSGB-BIO, China) was added for incubation at room temperature for another 1 h. Finally, a DAB kit (Boster Bio-Engineering Company, Wuhan, China) was used for color development according to the manufacturer's instructions. Photos were taken under a microscope (Zeiss, Oberkochen, Germany).

Histopathological staining

Tissues containing both macroscopic lesions and relatively normal regions in the two models were used to prepare histological slides. Briefly, fresh tissues were rapidly fixed in 4% paraformaldehyde fix solution for 48 h and then washed in slow running water overnight. After treatment in a gradient of alcohol, xylene and paraffin, tissues were embedded and cut. Section (5 µm) were stained with H&E solution to evaluate the pathological type, range, level of lesion and inflammatory cell infiltration. Photographs were taken using a microscope (Zeiss, Germany). Masson staining was conducted following the manufacturer's instructions (njjcbio, China).

Immunohistochemistry

The existence of *T. vaginalis* in infected tissues was determined by immunohistochemistry (IHC). Sections were dewaxed and hydrated, and the antigen was retrieved with citrate buffer solution (3.78 g citric acid monohydrate and 24.108 g sodium citrate in 1 L ddH_2O) maintaining in 92–95 °C for 10 min. After washing with PBS and treatment with 3% H_2O_2, sides were blocked with 5% BSA at 37 °C for 40 min. *T. vaginalis* in tissues was probed with rabbit anti-TV-α-actinin sera (1:1000) after

optimization and incubated at 37 °C for one hour. After being washed with PBS three times, slides were incubated with the anti-rabbit-HPR antibody (ZSGB-BIO, China) containing 3% H_2O_2 for another hour. Color detection was performed by using DAB (Sigma, USA) in the dark for 5 min and then stopped by distilled water. Sections were also counterstained with hematoxylin for 3 to 5 min. Photographs were taken using a fluorescent microscope (Zeiss, Germany). Additionally, parasites in the caseation caseation-like substance of mice from 30 dpi were also detected by H&E and IHC.

Statistical analysis

The graphics were constructed using GraphPad Prism 5 software. Statistical significance in the comparison of mean values and SEM was assessed by independent samples, and F tests and Student unpaired *t* tests were also performed by GraphPad Prism 5 software. Statistical significance was accepted at $P<0.05$. The parasite density in slides after IHC staining was quantified by scanning pathological sections with Image-Pro Plus software.

Results

Dose-dependent response to infection with *T. vaginalis*

To investigate the required inoculum for establishing an infection based on our parasite isolate, various numbers of *T. vaginalis* were inoculated into mice. Differences in survival percent are presented in Fig. 1A. When mice were intraperitoneally inoculated with 1×10^7 ($n=35$) parasites, a high mortality of approximately 97% (34/35) within 10 days post inoculation (dpi) was observed, which was defined as acute infection. Inoculation with 1×10^6 ($n=8$) parasites also resulted in a high mortality of approximately 90% (7/8), with one mouse dying at 6 dpi (acute infection) and the remaining 6 mice dying at 20–30 dpi, which was defined as chronic infection. Therefore, according to the onset and survival time, approximately 97% of mice with an inoculum of 1×10^7 developed acute infection, while 75% (6/8) of mice with an inoculum of 1×10^6 developed chronic infection.

Compared with mice in the control group (Figure S1A), acutely infected mice had a short latent period (approximately 2 days) and developed symptoms of decreased appetite, piloerection of fur, sloth, shakes and abdominal retraction. The clinical signs continued to deteriorate until death occurred over the next 2 to 4 days (Figure S1B). In the chronic infection group, a much longer latent period (approximately 7–14 days) and later chronic clinical progression were observed from mild illness to the last severe clinical symptoms, e.g., swollen enterocoelia and massive ascites accompanied by caseation-like lesions (Figures S1C and S1D). Mice with a lower inoculum of 1×10^5 ($n=8$) or 1×10^4 ($n=8$) *T. vaginalis* survived for over two months until being euthanized without visceral lesions. These results demonstrated that *T. vaginalis* infection by intraperitoneal inoculation in the mouse model is dose dependent.

Additionally, free parasites were quantified in the ascites of mice suffering acute and chronic infection. As shown in Fig. 1B, an average of 4.3×10^4 and 3.1×10^5 free *Trichomonas* were found in mouse ascites at 3 dpi and 5 dpi in the acute group, respectively. In ascites of the chronically infected mice, an average of 1.3×10^5, 4.0×10^6, 3.6×10^6 and 5.4×10^7 free *Trichomonas* were counted at 7, 14, 21 and 30 dpi, respectively. For the samples from 1 dpi in the acute group, 1 dpi and 3 dpi in the chronic group, the free *Trichomonas* in the mouse ascites were all below the direct counting threshold (1×10^4 per ml) with the hemocytometer.

Characterization of macroscopic lesions

To investigate organ damage caused by *T. vaginalis*, pathological scores were quantified in each group. In the acute group, mice showed obvious symptoms at 3 dpi (an average score of 10.0) and 5 dpi (an average score of 16.4) (Fig. 1C), in which lesions in the liver made the major contribution (an average score of 6.0 at 3 dpi and 10.8 at 5 dpi) (Fig. 1E). Spleen/pancreas/stomach (SPS) damage and ascites production also contributed to some scores (Fig. 1E).

In the chronic model, gradually increased scores indicated aggravated lesions in mice (Fig. 1D). As shown in Fig. 1F, the score at 3 dpi was mainly attributed to mild liver lesions (score of 3.6), slight damage of the peritoneum (score of 0.4) and the production of ascites (score of 1.2). After that, gradual deterioration occurred, e.g., scores on the diaphragmatic liver lesions continued to rise over time (Fig. 1F). Peritoneal (score of 4.4) and SPS (score of 7.6) damage was clearly observed at 21 dpi. At the last stage in the chronically infected mice, large lesions in multiple organs occurred, and the pathological scores reached almost 50, the full marks of the present study (Fig. 1D and F).

In both infected groups, obvious pathological damage appeared in the mouse liver and spleen. Therefore, they were chosen as representative organs for a more detailed exploration than other organs, including analysis of macroscopic and pathological changes, especially concerning the distribution of parasites displayed by IHC. As shown in Fig. 2, mouse livers seemed normal at 1 dpi in the acute group. Obvious yellow lesions in the liver and splenomegaly could be observed at 3 dpi. This was followed by the appearance of gradually enlarged lesions in the liver and spleen with fragmentary capsules at 5 dpi. In the chronic group (Fig. 2), although clinical manifestations were not yet observed at 3 dpi, small and yellow niduses could be found in the mouse liver. From 7 to 14 dpi, lesions in livers were extended, either at the margin

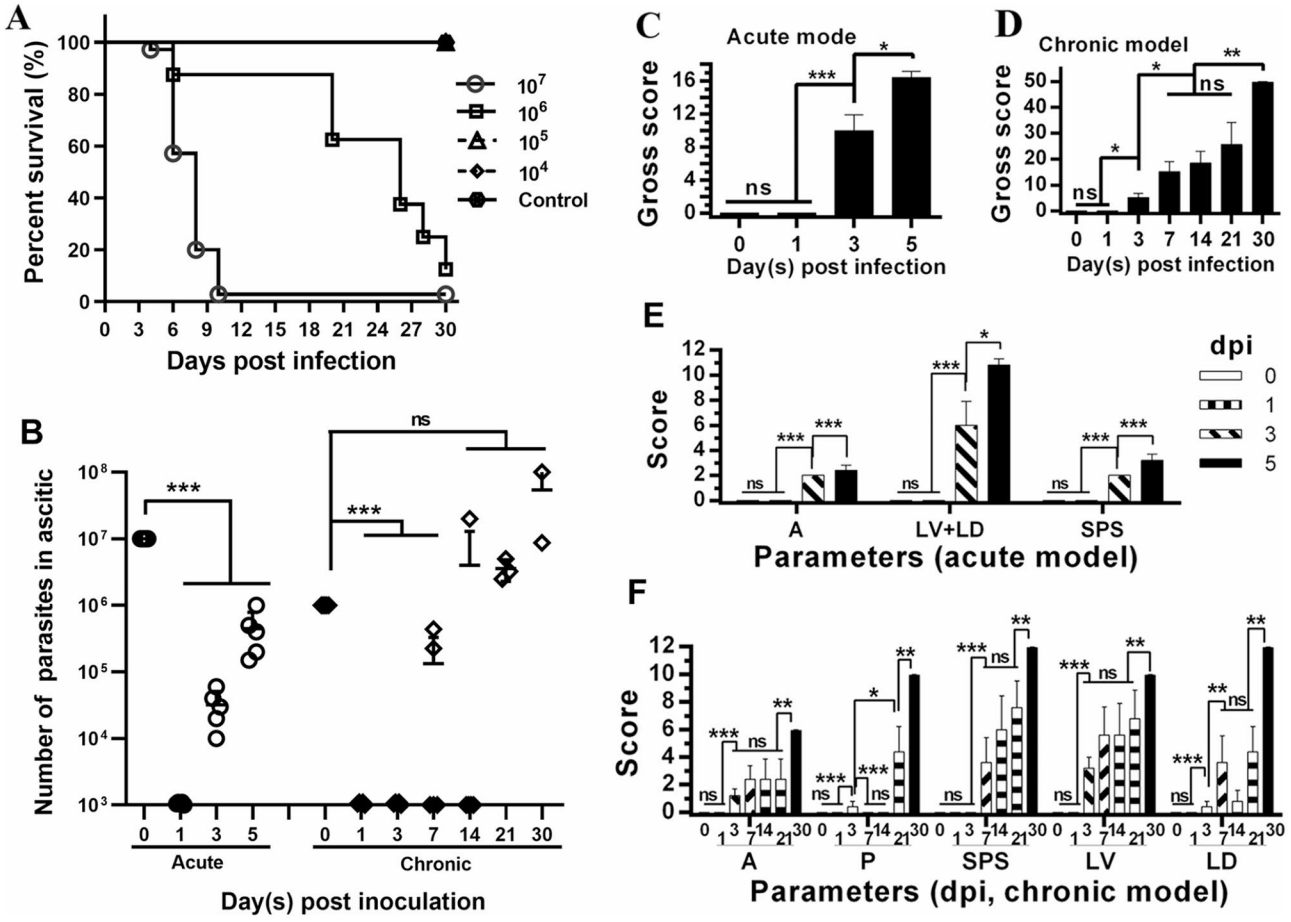

Fig. 1 The survival curve, parasite loads in ascites and pathological scores of mice infected with *T. vaginalis*. (**A**) The survival percentage of mice after intraperitoneal inoculation with the indicated numbers of *T. vaginalis*. (**B**) Free parasite numbers in mouse ascites. Mice with acute and chronic infection at the different time points were intraperitoneally injected with 2 ml precooled PBS, diluted ascites were collected, and parasite loads were determined by parasite density multiplied by the total volume of ascites ($n=5$). A total of five mice were excluded from this assay. Of these, two mice from the 21 dpi chronic group showed slight lesions, resulting in a low parasite loading below the direct counting threshold in ascites, and three mice in the chronic group died between 21–30 dpi before the timely collection of ascites. The total scores of pathological manifestations in mice acutely (**C**) or chronically (**D**) infected with *T. vaginalis* at different times. The scores of assigned indices in mice acutely (**E**) or chronically (**F**) infected with *T. vaginalis* at different times. A, ascites; P, peritoneum; SPS, spleen/pancreas/stomach; LV, visceral liver side; LD, diaphragmatic liver. Significant differences are indicated (* $p<0.05$ and *** $p<0.001$) by comparison with controls (0 d) (mean ± SEM), of which ns indicates not significant. A total of three mice were excluded from this assay. Of these, one mouse from the 14 dpi chronic group seemed not infected (pathological score = 0), and two mice in the chronic group died between 21–30 dpi before timely dissection

of the hepatic lobule or at the junction. Meanwhile, evident splenomegaly was observed. During the late phase of chronic infection (from 21 dpi to 30 dpi), the liver lesions became extensive and severe. The relatively normal hepatic tissue gradually decreased, and the whole liver looked pure red. The spleen capsule was broken and covered with ivory excretions. In both infected groups, splenomegaly was in accordance with a gradually increasing spleen coefficient (organ/body weight ratio) (Figure S2).

Alpha-actinin-based immunodetection of *T. vaginalis*

As shown in Fig. 3A, the anti-TV-α-actinin sera of three dilutions only specifically targeted the *T. vaginalis* antigens but not host cells in the dot-blot assay. The ICC results showed that TV-α-actinin proteins exist in the whole organism, including its flagella (Fig. 3B). The preliminary attempt of using anti-TV-α-actinin sera for immunodetection revealed an obvious advantage and clearer presentation of both free and amoeboid-formed *T. vaginalis* around or inside tissues by IHC staining (Fig. 3D and F) compared with common H&E staining (Fig. 3C and E). These results indicated that the anti-TV-α-actinin sera prepared by our laboratory could be used for immunodetection of *T. vaginalis* in animal tissues.

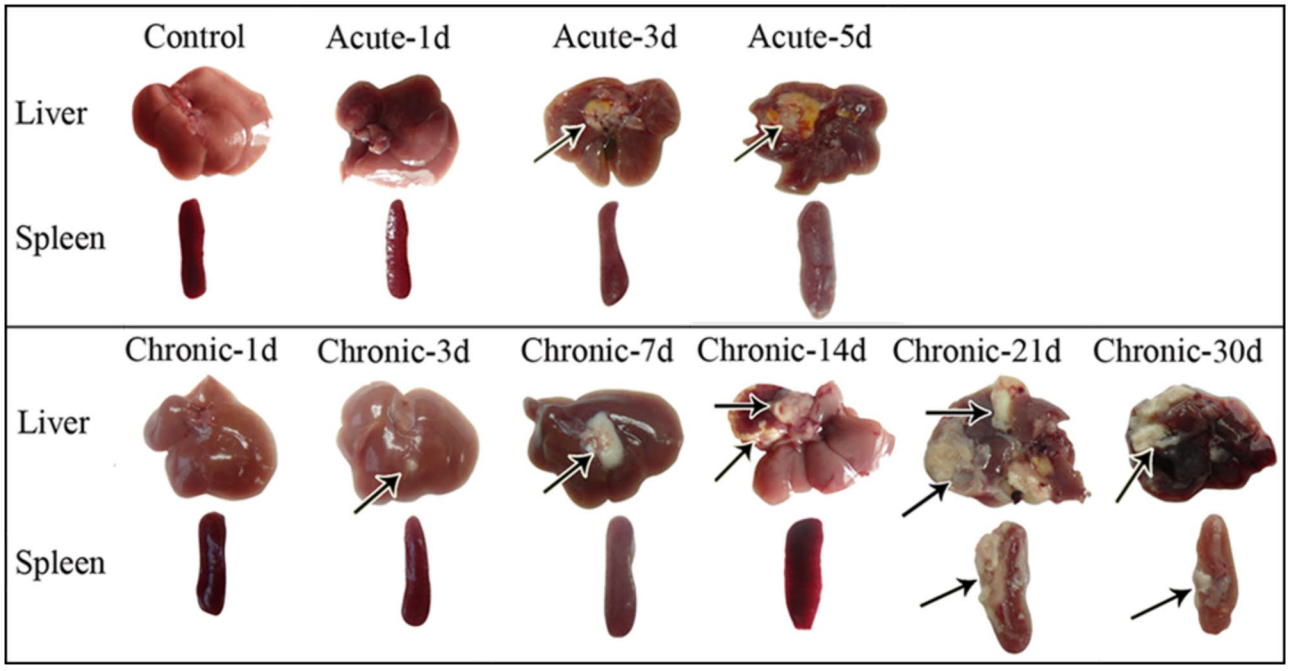

Fig. 2 Macroscopic lesions of livers and spleens in acutely and chronically infected mice by T. vaginalis. Lesions are indicated by black arrows

Characterization of pathological progression based on H&E and IHC staining

As shown in Fig. 4A1 and A2, livers from the control mice were characterized by intact hepatic lobes, hepatic cord, and hepatic sinus but without *T. vaginalis* (Fig. 4A3). In the acute group, liver structures from mice at 1 dpi appeared structurally normal (Fig. 4B1). Despite this, small spotted regions and foci of necrosis were found in some hepatic lobules with inflammatory cell infiltration (Fig. 4B2 and B3). However, *T. vaginalis* was not identified around these foci (Fig. 4B4). At 3 dpi (Fig. 4C1 and C2), there was patchy necrosis in the liver, where hepatocytes had dissolved, leaving fragmented remains of hepatocyte nuclei. The peripheral hepatocytes around the necrotic regions had become swollen and degenerated. Inflammatory cell infiltration and abscesses caused by necrotic inflammatory cells were found around the necrotic focus and peripheral areas. According to the immunohistochemical staining, a mass of *T. vaginalis* appeared in a palisade arrangement around the necrotic foci and their perimeter zones (Fig. 4C3). At 5 dpi, the necrotic foci in the liver had become more extensive, and larger-scale necrosis was accompanied by many neutrophils and eosinophilic granulocytes (Fig. 4D1 and D2). The intrahepatic vascular regions showed evident angiectasis and hyperemia (Fig. 4D1). Intensive *T. vaginalis* gathered along the junctions of necrotic and relatively normal areas (Fig. 4D3 and D4). The density of *T. vaginalis* in the necrotic areas reached approximately 9.8% at 3 dpi and increased to 11.5% at 5 dpi (Fig. 4E).

In the control group, spleen tissues of mice were characterized by an intact capsule, normal splenic sinuses and corpuscles (Fig. 5A1 and A2) but without *T. vaginalis* (Fig. 5A3). At 1 dpi in the acute group, red pulp and white pulp could still be clearly distinguished (Fig. 5B1), but some neutrophils and multinucleated giant cells (MGCs) were found in the red pulp (Fig. 5B2). *T. vaginalis* was not yet found in the spleen pathology sections (Fig. 5B3). By 3 dpi, the histological structure of the spleen had become disordered. The demarcation between red and white pulp was blurred, and an increasing number of MGC appeared (Fig. 5C1 and C2). Lymphocytes in the white pulp also underwent apoptosis (Fig. 5C3). Small patchy necrotic regions occurred with inflammatory cell infiltration at the margins of the spleen (Fig. 5C4). *T. vaginalis* was distributed on the surface of the spleen capsule like a fence (Fig. 5C5). At 5 dpi, the spleen structure was obviously disordered, with large patchy areas of disintegrating cells and necrosis (Fig. 5D1). The demarcation of red pulp and white pulp had completely broken down. In the necrotic foci, there were abscesses consisting of neutrophils, eosinophils, nuclear debris and *T. vaginalis.* Many MGCs still existed, and the blood vessels of the spleen were dilated and showed hyperemia (Fig. 5D1 and D2). The results of the IHC staining revealed that a large number of *T. vaginalis* were distributed in the abscesses as well as in the peripheral splenic tissue (Fig. 5D3).

Within the early stage of the chronic group (from 1 dpi to 3 dpi), some spotted and necrotic foci first appeared in the mouse liver (1 dpi), where the hepatocytes began disintegrating with infiltration of some inflammatory cells

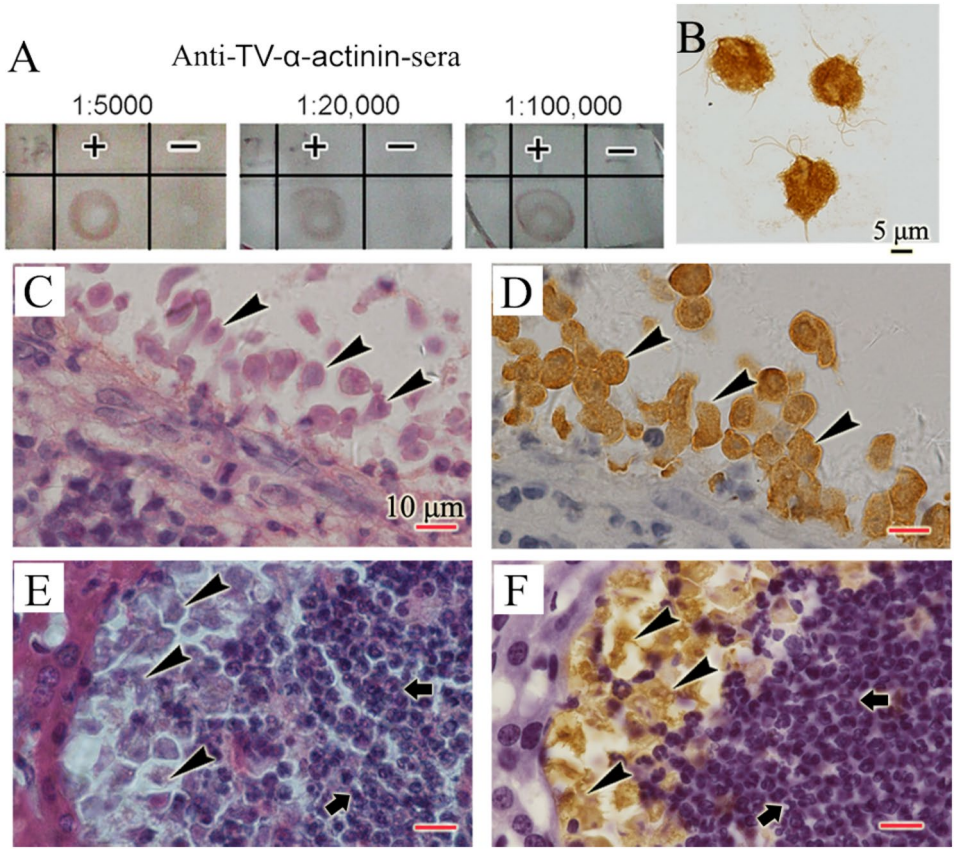

Fig. 3 Confirmation of the specificity and applicability of anti-TV-α-actinin sera for immunodetection. (**A**) Specificity assessment was performed using anti-TV-α-actinin sera at different concentrations by dot blot. "+" indicates the whole cell antigens prepared by *T. vaginalis*, "-" indicates the whole cell antigens prepared by splenocytes of uninfected mice. (**B**) The intracellular localization of α-actinin in *T. vaginalis* was determined using anti-TV-α-actinin sera (1:1000 after optimization) by ICC assay. (**C** and **D**) The relatively typical *T. vaginalis* attached to the surface of the mouse liver was observed by H&E staining and IHC (anti-TV-α-actinin sera, 1:1000), respectively. (**E** and **F**) Ameboid-like *T. vaginalis* invading the mouse liver and surrounding inflammatory cells were observed by H&E staining and IHC (anti-TV-α-actinin sera, 1:1000). The black arrows indicate inflammatory cells; arrowheads indicate *T. vaginalis*

(Fig. 6A1 and A2) but without *T. vaginalis* (Fig. 16A3). Then, the livers from 40% (2/5) of the mice (3 dpi) showed some small patchy necrosis beside the small nidus, in which a large number of inflammatory cells were observed (Fig. 6B1 and B2), but only a low density of *T. vaginalis* (0.3%) was observed (Fig. 6B3 and G). In the middle stage of the chronic infection group (from 7 to 21 dpi), individual and confluent necrosis appeared in the liver and gradually expanded. In those areas, inflammatory cells, including neutrophils and eosinophils, as well as their lysates, formed obvious hepatapostema (Fig. 6C1, C2, D1, D2, E1 and E2). Hepatocytes around the junction of necrosis and relatively normal liver tissue had transformed into severe edema. Meanwhile, a large number of parasites were observed to gather in or around the abscess (Fig. 6C3, D3 and E3). Compared to the first and third day, parasite density in the liver necrotic areas of this stage significantly increased up to 5.5–6.2% (Fig. 6G). During the last stage of the chronic model, severe hepatapostema was observed in the mice, and very little normal liver tissue remained. The infiltrated inflammatory cells still mainly consisted of neutrophils and eosinophils (Fig. 6F1-F3). A large number of *T. vaginalis* gathered in or around the necrotic abscesses (Fig. 6F4 and G). The parasite density (8.1%) in the necrotic areas was even closer to that of the late stage in the acute infection group (Figs. 4E and 6G). Part of the liver also became fibrotic (Figure S3). There was also a mass of caseation-like substance that filled the enterocoelia, especially around the liver. Many *T. vaginalis* and cell debris without nuclei were found by optical microscopy and immunostaining (Figures S1D-F).

In the chronic group, spleen pathological changes were also significant. Within the first 3 dpi, spleen tissues looked normal but contained some MGCs (Fig. 7A1, A2, B1 and B2). Thereafter, the structure of the spleen (from 7 to 14 dpi) gradually became disordered, and demarcation between the red pulp and white pulp became blurred. Many MGCs were found in the red pulp, lymphocytes in the white pulp were reduced, and some necrotic foci were observed (Fig. 7C1, C2 and D1, D2). *T. vaginalis* was not observed before 21 dpi (Fig. 7A3, B3, C3 and D3). From

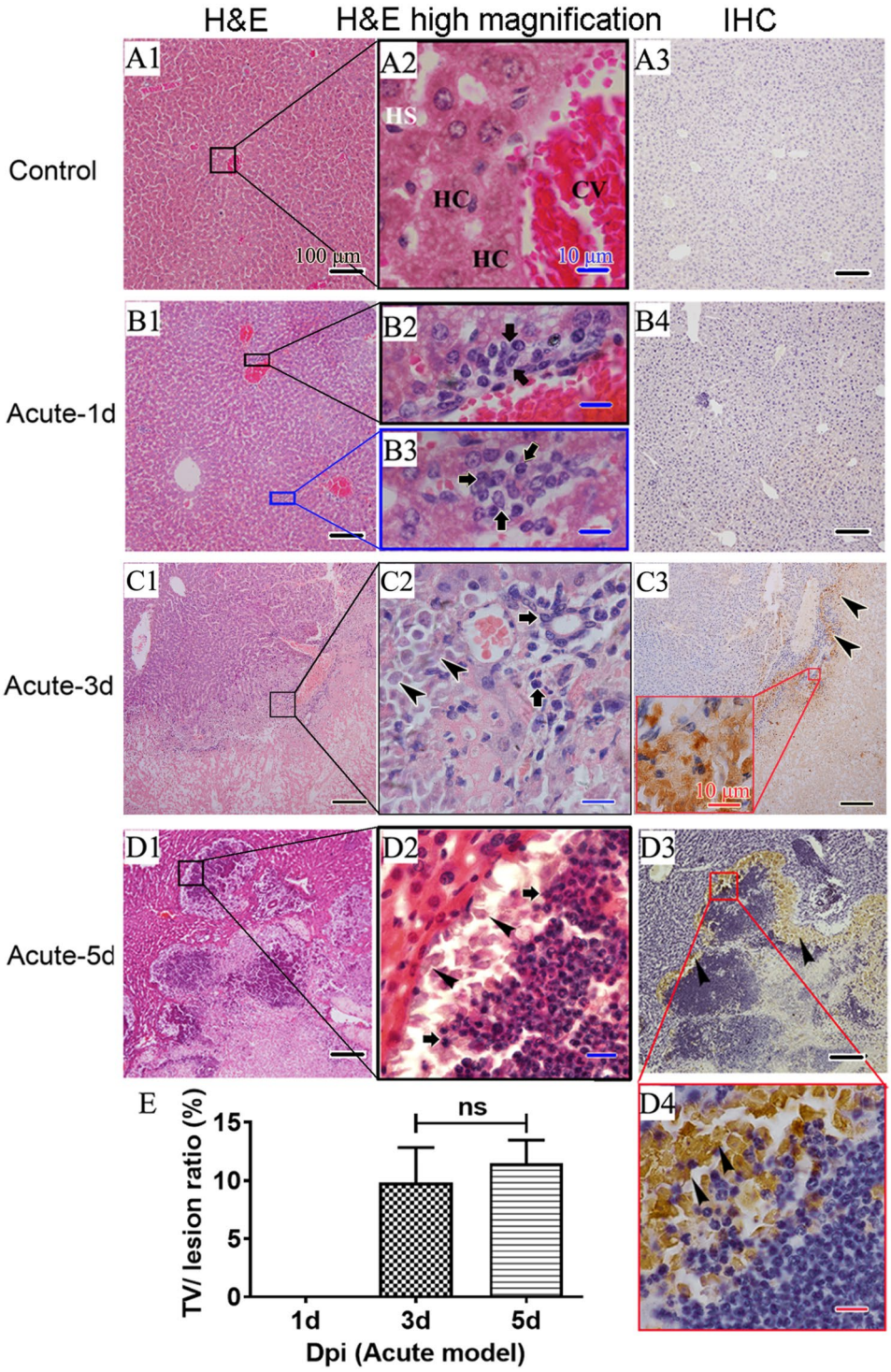

Fig. 4 H&E and IHC staining of liver sections from mice acutely infected with *T. vaginalis* at different time points. (**A1**-**A3**) Control. (**B1**-**B4**) Acute-1d. (**C1**-**C3**) Acute-3d. (**D1**-**D4**) Acute-5d. (**E**) The parasite burden was shown as the ratio of the occupied area of *T. vaginalis* to the lesion area. Approximately 0.25 to 1 cm2 of area was scanned for the calculation of the TV occupied/lesion ratio. The data shown are the means ± SEMs. CV: central veins; HS: hepatic sinusoid; HC: hepatic cord; black arrows indicate inflammatory cells; arrowheads indicate *T. vaginalis*; ns: not significant. The black scale bars indicate 100 μm under 10× magnification, and the blue scale bars and red scale bars indicate 10 μm under 100× magnification. The magnified regions are outlined by rectangular boxes in the same color

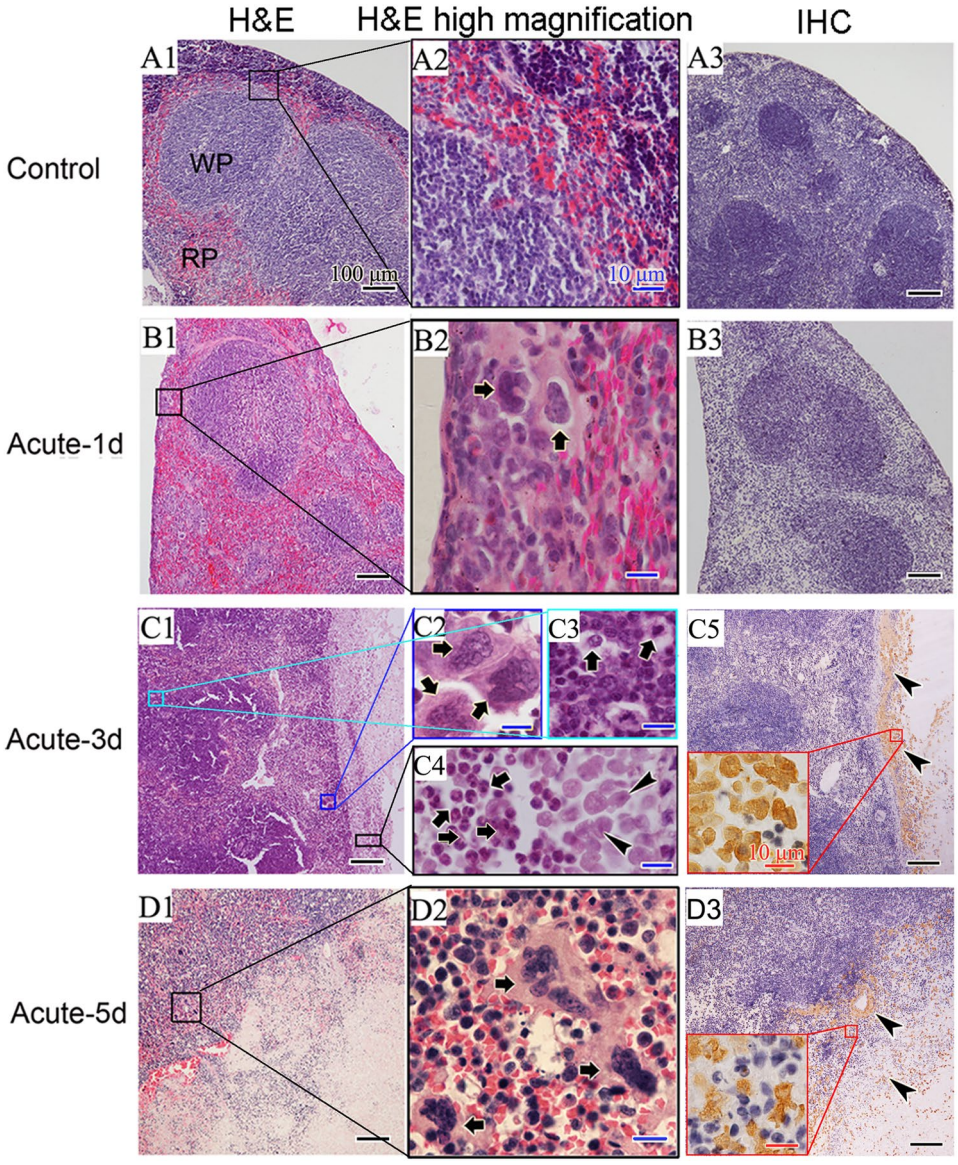

Fig. 5 H&E and IHC staining of spleen sections from mice acutely infected with *T. vaginalis* at different time points. (**A1**-**A3**) Control. (**B1**-**B3**) Acute-1d. (**C1**-**C5**) Acute-3d. (**D1**-**D3**) Acute-5d. RP: red pulp; WP: white pulp; black arrows indicate inflammatory cells; arrowheads indicate *T. vaginalis*. The black scale bars indicate 100 μm under 10× magnification, and the blue scale bars and red scale bars indicate 10 μm under 100× magnification. The magnified regions are outlined by rectangular boxes in the same color

21 dpi on, *T. vaginalis* were found to gather around the spleen capsule, which had been broken and was no longer integral (Fig. 7E1-E4). At 30 dpi, obvious abscesses were found in mouse spleens. Many *T. vaginalis* (Fig. 7F3) and inflammatory cells consisting of lymphocytes, neutrophil granulocytes and monocytes (Fig. 7F1 and F2) filled in the large patchy necrotic area.

Pathological changes in other organs in mice

When compared with the control group (Figure S4A), vasodilatation and hyperemia were observed in the kidneys of acutely infected mice at 5 dpi (Figure S4B). The tubules were slightly edematous, whereas small foci of inflammatory cell infiltration were observed in the kidneys at 30 days after chronic infection (Figure S4C). When compared with the control group (Figure S4D), the IHC results showed that there were *Trichomonas* aggregation and inflammatory cell infiltration on the renal capsule surface at both time points (Figures S4E and S4F).

When compared with the control group (Figure S5A), vasodilatation and hyperemia were also observed in the lung tissue of acutely infected mice at 5 dpi (Figure S5B). For chronically infected mice at 30 dpi, the lung tissue was edematous, the blood vessels were dilated and hyperemic, and more pink edematous fluid was observed in the alveolar cavity (Figure S5C). The IHC results showed that

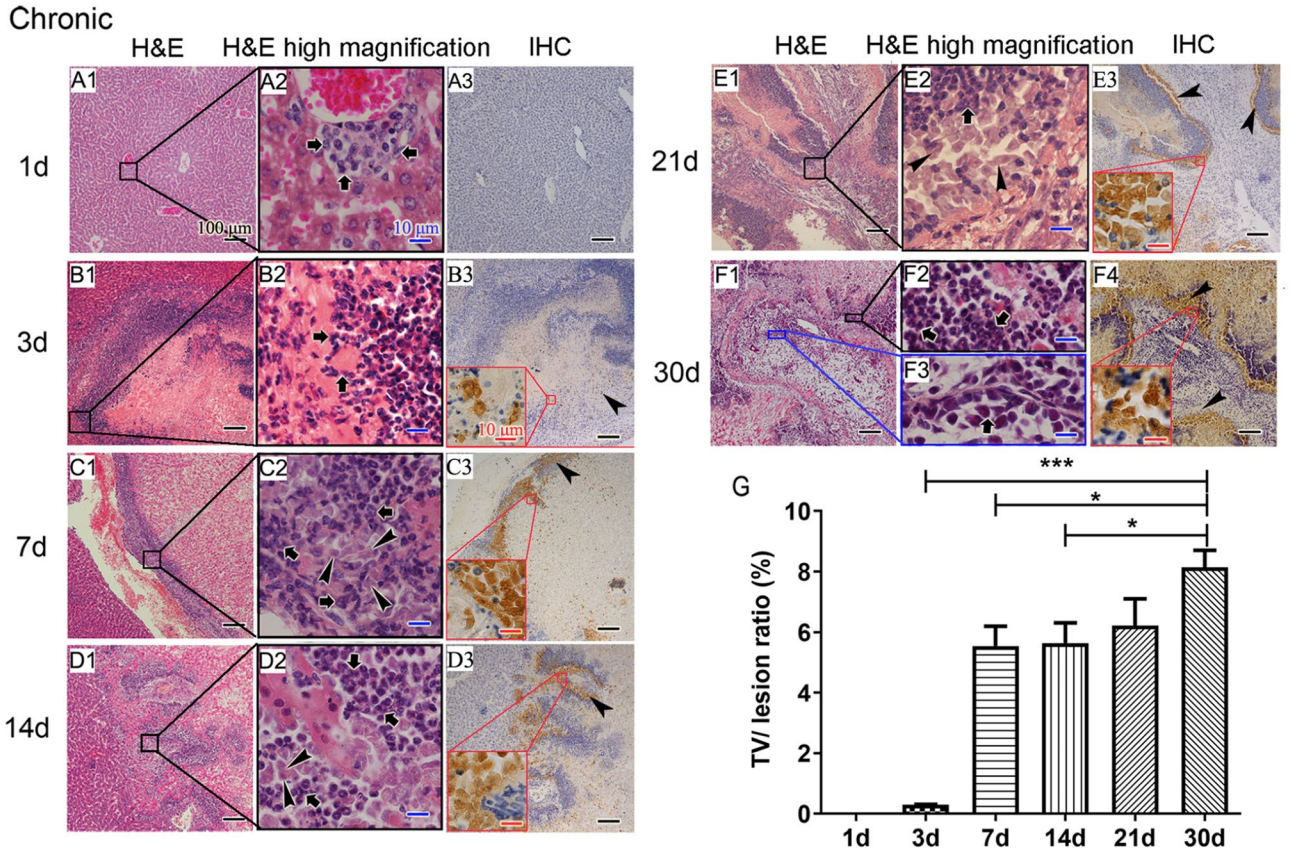

Fig. 6 H&E and IHC staining of liver sections from mice chronically infected with *T. vaginalis* at different time points. (**A1**-**A3**) Chronic-1d. (**B1**-**B3**) Chronic-3d. (**C1**-**C3**) Chronic-7d. (**D1**-**D3**) Chronic-14d. (**E1**-**E3**) Chronic-21d. (**F1**-**F4**) Chronic-30d. (**G**) The intensity of parasite burden is shown by the ratio of the occupied area of *T. vaginalis* to the lesion area. Approximately 0.25 cm2 to 1 cm2 of area was scanned for the calculations of the TV occupied/lesion ratio. The data shown are the means ± SEMs, * ($p < 0.05$) and *** ($p < 0.001$). Black arrows indicate inflammatory cells; arrowheads indicate *T. vaginalis*. The black scale bars indicate 100 μm under 10× magnification, and the blue scale bars and red scale bars indicate 10 μm under 100× magnification. The magnified regions are outlined by rectangular boxes in the same color

no *Trichomonas* was observed in the mice of the control group (Figure S5D) but existed on the bronchial mucosal surface of the acutely infected mice at 5 dpi (Figure S5E) and the alveolar space of chronically infected mice at 30 dpi (Figure S5F). Additionally, *T. vaginalis* was also detected in the blood vessels or vascular walls of mouse livers from different dpi in both the acute (Figure S6A) and chronic (Figure S6B) groups.

Discussion

Peritoneal infection of *T. vaginalis* in mice is one of the most common animal models for research on this parasite. A deeper understanding of the extensively characterized progression and pathologic features of this model, in our opinion, will be beneficial to its better use in future studies. Therefore, a dynamic observation of the macroscopic, histological lesions and *T. vaginalis* distribution, especially when diagnosed based on TV-α-actinin-specific immunological detection in the peritoneal infection model, was conducted in the present study.

According to previous studies, several possible influencing factors have been found to be involved in the establishment of this model, such as the susceptibility of mouse strains, the inoculum size of parasites and the infection duration based on the different isolates. Therefore, these elements were first considered in the present study. There were three mouse strains including Swiss, BALB/c and C57BL/6 have been found all susceptible to the *T. vaginalis* isolate used in the present study before. Of which, Swiss mice, as far as we know, were rarely reported to be used in this model. Therefore, Swiss mice were chosen in the following study with the hope of providing more information on the available hosts for intraperitoneal model of *T. vaginalis* infection.

In accordance with the results in previous studies [10, 24], inoculation of 1×10^7 and 1×10^6 parasites could cause death in mice, and the average survival time was approximately 7 days and 3 weeks, respectively. However, inoculation of 1×10^5 or 1×10^4 parasites failed to result in clinical signs in Swiss mice even when the observation time was finally extended to two months. This indicated

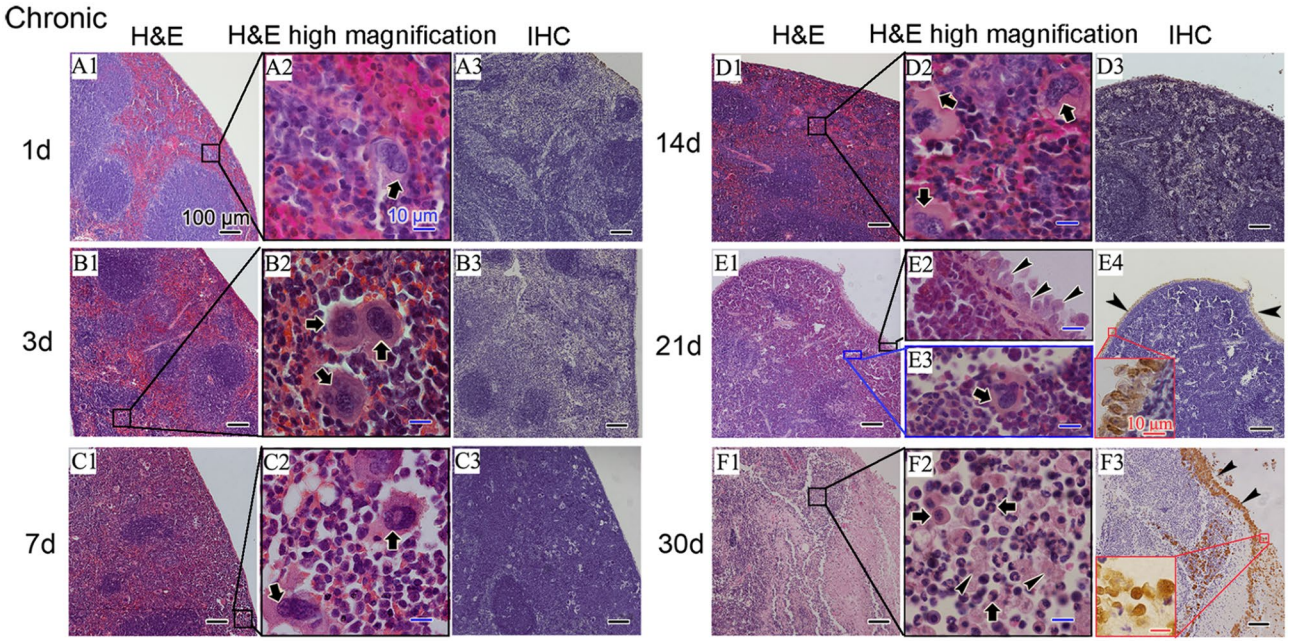

Fig. 7 H&E and IHC staining of spleen sections from mice chronically infected with *T. vaginalis* at different time points. (**A1**-**A3**) Chronic-1d. (**B1**-**B3**) Chronic-3d. (**C1**-**C3**) Chronic-7d. (**D1**-**D3**) Chronic-14d. (**E1**-**E4**) Chronic-21d. (**F1**-**F3**) Chronic-30d. Black arrows indicate inflammatory cells; arrowheads indicate *T. vaginalis*. The black scale bars indicate 100 μm under 10× magnification, and the blue scale bars and red scale bars indicate 10 μm under 100× magnification. The magnified regions are outlined by rectangular boxes in the same color

that the infection of *T. vaginalis* and lethality in mice were parasite number-dependent. Additionally, the relatively long latent period (approximately 2 weeks) but severe symptoms and death of mice in the later stage reminded us that the infection duration was closely related to the parasite number inoculated. Therefore, researchers had better optimize the observation period and parasite number inoculated according to different isolates if needed before using this model.

The present study also reconfirmed the proliferation of *T. vaginalis* in mice and their invasion and metastasis processes, as reported in a previous document [10]. The increase in free *T. vaginalis* in mouse ascites from less than 10^4 on the early dpi to approximately 3×10^5 (acute) or nearly 10^7 (chronic) in mouse ascites before being executed indicated the proliferative capacity of this parasite in mice. Just as viewpoint by Kulda [10], many *Trichomonas* were initially eliminated by innate immune responses, especially by macrophages, which are considered an important line of defense to kill *T. vaginalis* in vivo [32]. After comparing the acute and chronic models and gaining a deeper understanding of this process, we propose the following opinion as a supplement: although the host has its original scavenging (immunoclearance) ability to kill the pathogen, this protection will become insufficient once the number of parasites reaches a certain threshold, and beyond this threshold, remaining *T. vaginalis* will gradually proliferate, and the host will then become sick. In the acute infection model, it is likely that more *T. vaginalis* will be able to escape from the initial host innate immune attack than that in the chronic mouse model. As a result, a larger number of parasites remaining (beyond the initial immunoclearance threshold of the mice) could cause acute lesions, resulting in the rapid death of the infected mice before massive proliferation of *T. vaginalis* occurs. Conversely, after the first conflict between *T. vaginalis* and the host immune response in chronically infected mice, the remaining parasites in the abdominal cavity would be quite limited in number, resulting in a gradually slow invasion of the internal organs. Therefore, a more moderate pathological process was observed until rapid proliferation occurred. Following this, organ tropism may enable the spreading of *T. vaginalis*. Additionally, parasites can invade or adhere to the internal organs of mice due to their strong adhesive ability [26, 33], which might be another reason for the decrease in free *T. vaginalis* in mouse ascites. This was also in accordance with our results that the average parasite density in the necrotic areas of mouse livers from the chronic group (0.3%) was significantly lower than that found in the acute group (9.8%) at 3 dpi, indicating that fewer parasites had escaped from the mouse immunoclearance in the chronic group and invaded the mouse livers.

As one of the most immunogenic trichomonad proteins, TV-α-actinin has been widely used as the diagnostic target of trichomoniasis. For example, in an investigation of associations between *T. vaginalis* and

prostate cancer, a recombinant *T. vaginalis* α-actinin IgG ELISA was used to explore serologic evidence of a history of trichomoniasis [3]. Several related studies also revealed that epitopes of the highly immunogenic TV-α-actinin were serodiagnostic targets for both women and men. The point-of-care serodiagnostic test for *T. vaginalis* has been developed based on this protein [29, 34–36]. Similarly, TV-α-actinin used in the present study clearly presented a more visualized pathological process by combining H&E with IHC staining in mice at different dpi, especially for the localization of parasites. As we know, *T. vaginalis* usually transforms from its typical pear shape into an amoeboid-like shape once in contact with host cells [26]. These relatively inactive and atypically shaped *T. vaginalis* are often hidden among somatic cell clusters, making recognition of them relatively difficult in tissue slice by light microscopy [37, 38] even when stained with H&E solution. Therefore, the observer's technical expertise is usually highly required. Luckily, the high specificity of the anti-TV-α-actinin sera guaranteed no cross reactivity between our sera with α-actinin homologs in humans [28, 29], confirming the reliability of this method for the diagnosis of *T. vaginalis* in mouse organs.

As shown by H&E and IHC staining, hepatic pathological changes in both the acute and chronic groups were gradually aggravated and characterized by disintegrating hepatocytes with cell debris in the necrotic area, inflammatory infiltrates (e.g., lymphocytes, eosinophils, monocytes and neutrophils) and the presence of a large number of parasites distributed as a fence between the lesion and relatively normal areas.

Particularly, neutrophils were found dramatically swarming around the parasites. This is consistent with the influx of neutrophils to the vaginal mucosa [39] of trichomoniasis patients. As we know, human neutrophils have been revealed to attack *T. vaginalis in vitro* [40]. A very interesting study found that neutrophils could rapidly kill *T. vaginalis* in a manner named "trogocytosis" within approximate 15 min. In which, neutrophils surround and take an average of 3 to 8 "bites" on the membrane of only live *T. vaginalis* (using phagocytosis for dead parasites) before their death. And this novel mechanism for *T. vaginalis* killing is mediated by antibody-Fc receptor and neutrophils serine proteas in a dose-dependent and contact-dependent manner [40] as well as complement receptor 3 [41]. Although recent studies have not yet tested whether this neutrophils-trogocytosis manner in *T. vaginalis* killing occurs in vivo [42] and it was also failed to be observed in the current study due to the limitation of detection methods, research that used the electron microscopy and intravital imaging to successfully demonstrate the trogocytic killing of cancer cells by neutrophil in vivo [43], gives us some confidence to use animal models, such as the peritoneal infection model of *T. vaginalis*, to verify this phenomenon in the future. For the spleen, in accordance with earlier reports [10], a gradually increasing frequency of multinuclear giant cells (MGCs) was dramatically observed in pathological sections of mouse spleen along with infection progression, indicating that the production of MGCs is a typical feature of this model. Bal and colleagues [44] considered that these MGCs consisted of several immune cells as a response to pathogen attack. According to IHC assay, *T. vaginalis* first sticked to the capsule of the spleen and then invaded the interior, causing extensive necrosis accompanied by large amounts of inflammatory cell infiltration. Surprisingly, unlike the severe damage found in the livers and spleens of the infected mice, only mild lesions and a relatively small amount of *T. vaginalis* were observed in other organs, such as the kidneys and lungs, at the late stages in both acutely and chronically infected mice. It seems that *T. vaginalis* has a preference for certain organs in abdominal cavity, especially for liver. This is, perhaps, due to the differences in their microenvironment components. However, the in-depth and accurate mechanisms about this organ preference of *T. vaginalis* invasion need further exploration.

Interestingly, a spot of *T. vaginalis* were also detected in the hepatic vascular system by using immune staining, even in locations far from the foci of infection, although the number of parasites in hepatic blood was limited. We doubt whether this perhaps proposed a possibility that *T. vaginalis* could spread to other organs via the blood circulation from the original infection site, as the earlier report that trichomonads could occasionally survive in human blood [45]. This probably also indicates another possibility that *T. vaginalis* could migrate to other organs to establish the ectopic infection by this way. Actually, some clinical studies have reported that *T. vaginalis* migrated into the human abdominal cavity and caused ascites production, or perihepatic abscess and perinephric abscess, occasionally [46, 47]. Therefore, perhaps intraperitoneal infection actually reflects an occasionally natural infection route and research on this model may also be beneficial for understanding ectopic infection of *T. vaginalis* in humans. Even so, it is, after all, not a routine infection route of *T. vaginalis* in the human body, indicating that the usage of intraperitoneal infection model also has certain limitations compared with the vaginal model. For example, for exploring the effect of vaginal microbiota and vaginal mucosal immunity on the establishment of *T. vaginalis* infection and the interaction of different sexually transmitted pathogens in the vagina, only the vaginal model can be used due to the different microenvironment between the abdominal cavity and the vagina. Therefore, the choice of mouse models should be objective and rigorous.

Conclusions

In summary, the present study focused on further revealing the progression and pathologic features of intraperitoneal infection of *T. vaginalis* in mice, especially by means of TV-α-actinin-based immunological detection. The clearer and more detailed presentation of the pathologic characteristics of this model, in our opinion, will benefit its better use in future studies.

Supplementary Information

The online version contains supplementary material available at https://doi.org/10.1186/s12879-024-10041-8.

Supplementary Material 1

Acknowledgements
The authors would like to thank all members in the authors' laboratories who provided great help when the work was carried out and the data were analyzed.

Author contributions
ZR. L, YT. X and DH. L designed the study and wrote the draft. YT. X and CX. Z carried out the experimental work. YT. X, CX. Z, DH. L, P. T, G. H and ZR. L analyzed the data. All authors have approved the final manuscript.

Funding
This work was supported by grants from the National Natural Science Foundation of China (ZRL, grant number #31472058 and 31720103918). The funders had no role in the study design, data collection and analysis, decision to publish, or preparation of the manuscript.

Data availability
The datasets used and/or analyzed during the current study are available from the corresponding author on reasonable request.

Declarations

Ethics approval and consent to participate
This study was approved by the Institutional Review Board for Animal Care of Sun Yat-Sen University, Guangdong, China. The ethics approval numbers are #31472058 and 31720103918.

Consent for publication
Not applicable.

Competing interests
The authors declare no competing interests.

Received: 19 March 2024 / Accepted: 2 October 2024
Published online: 17 October 2024

References

1. WHO Guidelines Approved by the Guidelines Review Committee. In: Recommendations for the treatment of Trichomonas vaginalis, Mycoplasma genitalium, Candida albicans, bacterial vaginosis and human papillomavirus (anogenital warts). edn. Geneva: World Health Organization © World Health Organization 2024.; 2024.
2. Laga M, Manoka A, Kivuvu M, Malele B, Tuliza M, Nzila N, et al. Non-ulcerative sexually transmitted diseases as risk factors for HIV-1 transmission in women: results from a cohort study. Aids. 1993;7(1):95–102.
3. Sutcliffe S, Giovannucci E, Alderete JF, Chang TH, Gaydos CA, Zenilman JM, et al. Plasma antibodies against Trichomonas Vaginalis and subsequent risk of prostate cancer. Cancer Epidemiol Biomarkers Prev. 2006;15(5):939–45.
4. Stark JR, Judson G, Alderete JF, Mundodi V, Kucknoor AS, Giovannucci EL, et al. Prospective study of Trichomonas vaginalis infection and prostate cancer incidence and mortality: Physicians' Health Study. J Natl Cancer Inst. 2009;101(20):1406–11.
5. Cotch MF, Pastorek JG 2nd, Nugent RP, Hillier SL, Gibbs RS, Martin DH, et al. Trichomonas vaginalis associated with low birth weight and preterm delivery. The vaginal infections and Prematurity Study Group. Sex Transm Dis. 1997;24(6):353–60.
6. Smith LM, Wang M, Zangwill K, Yeh S. Trichomonas vaginalis infection in a premature newborn. J Perinatol. 2002;22(6):502–3.
7. Meites E. Trichomoniasis: the neglected sexually transmitted disease. Infect Dis Clin North Am. 2013;27(4):755–64.
8. Corbeil LB. Use of an animal model of trichomoniasis as a basis for understanding this disease in women. Clin Infect Dis. 1995;21(Suppl 2):S158–61.
9. Cobo ER, Eckmann L, Corbeil LB. Murine models of vaginal trichomonad infections. Am J Trop Med Hyg. 2011;85(4):667–73.
10. Kulda J. Employment of experimental animals in studies of Trichomonas Vaginaiis Infection[M]//Trichomonads parasitic in humans. New York: Springer; 1990. pp. 112–54.
11. Garber GE, Lemchuk-Favel LT. Association of production of cell-detaching factor with the clinical presentation of Trichomonas vaginalis. J Clin Microbiol. 1990;28(11):2415–7.
12. Xie YT, Gao JM, Wu YP, Tang P, Hide G, Lai DH, et al. Recombinant α-actinin subunit antigens of Trichomonas Vaginalis as potential vaccine candidates in protecting against trichomoniasis. Parasit Vectors. 2017;10(1):83.
13. Zhang Z, Li Y, Wang S, Hao L, Zhu Y, Li H, et al. The molecular characterization and immunity identification of Trichomonas Vaginalis adhesion protein 33 (AP33). Front Microbiol. 2020;11:1433.
14. Hernández H, Sariego I, Garber G, Delgado R, López O, Sarracent J. Monoclonal antibodies against a 62 kDa proteinase of Trichomonas vaginalis decrease parasite cytoadherence to epithelial cells and confer protection in mice. Parasite Immunol. 2004;26(3):119–25.
15. Meneses-Marcel A, Marrero-Ponce Y, Ibáñez-Escribano A, Gómez-Barrio A, Escario JA, Barigye SJ, et al. Drug repositioning for novel antitrichomonas from known antiprotozoan drugs using hierarchical screening. Future Med Chem. 2018;10(8):863–78.
16. Nogal-Ruiz JJ, Gómez-Barrio A, Escario JA, Montero-Pereira D, Martínez-Fernández AR. Effect of piroxicam, metamizol, and S-adenosylmethionine in a murine model of experimental trichomoniasis. Parasite. 2005;12(1):79–83.
17. Nogal-Ruiz JJ, Gómez-Barrio A, Escario JA, Martínez-Fernández AR. Effect of Anapsos in a murine model of experimental trichomoniasis. Parasite. 2003;10(4):303–8.
18. Nogal-Ruiz JJ, Gómez-Barrio A, Escario JA, Martínez-Fernández AR. Modulation by Polypodium leucotomos extract of cytokine patterns in experimental trichomoniasis model. Parasite. 2003;10(1):73–8.
19. Gómez-Barrio A, Nogal-Ruiz JJ, Montero-Pereira D, Rodríguez-Gallego E, Romero-Fernandez E, Escario JA. Biological variability in clinical isolates of Trichomonas vaginalis. Mem Inst Oswaldo Cruz. 2002;97(6):893–6.
20. Gold D. Trichomonas vaginalis: strain differences in adhesion to plastic and virulence in vitro and in vivo. Parasitol Res. 1993;79(4):309–15.
21. El-Gayar EK, Mokhtar AB, Hassan WA. Molecular characterization of double-stranded RNA virus in Trichomonas Vaginalis Egyptian isolates and its association with pathogenicity. Parasitol Res. 2016;115(10):4027–36.
22. Rangel-Mata FJ, Ávila-Muro EE, Reyes-Martínez JE, Olmos-Ortiz LM, Brunck ME, Arriaga-Pizano LA, et al. Immune cell arrival kinetics to peritoneum and role during murine-experimental trichomoniasis. Parasitology. 2021;148(13):1624–35.
23. Ibáñez-Escribano A, Nogal-Ruiz JJ, Pérez-Serrano J, Gómez-Barrio A, Escario JA, Alderete JF. Sequestration of host-CD59 as potential immune evasion strategy of Trichomonas vaginalis. Acta Trop. 2015;149:1–7.
24. Reardon LV, Ashburn LL, Jacobs L. Differences in strains of Trichomonas Vaginalis as revealed by intraperitoneal injections into mice. J Parasitol. 1961;47:527–32.
25. Nogal Ruiz JJ, Escario JA, Martinez Diaz RA, Gomez Barrio A. Evaluation of a murine model of experimental trichomoniasis. Parasite. 1997;4(2):127–32.
26. Arroyo R, González-Robles A, Martínez-Palomo A, Alderete JF. Signalling of Trichomonas Vaginalis for amoeboid transformation and adhesion synthesis follows cytoadherence. Mol Microbiol. 1993;7(2):299–309.
27. Addis MF, Rappelli P, Delogu G, Carta F, Cappuccinelli P, Fiori PL. Cloning and molecular characterization of a cDNA clone coding for Trichomonas Vaginalis alpha-actinin and intracellular localization of the protein. Infect Immun. 1998;66(10):4924–31.

28. Addis MF, Rappelli P, De Pinto AM, Rita FM, Colombo MM, Cappuccinelli P, et al. Identification of Trichomonas Vaginalis alpha-actinin as the most common immunogen recognized by sera of women exposed to the parasite. J Infect Dis. 1999;180(5):1727–30.
29. Neace CJ, Alderete JF. Epitopes of the highly immunogenic Trichomonas vaginalis α-actinin are serodiagnostic targets for both women and men. J Clin Microbiol. 2013;51(8):2483–90.
30. Xiao JC, Xie LF, Fang SL, Gao MY, Zhu Y, Song LY, et al. Symbiosis of Mycoplasma hominis in Trichomonas Vaginalis may link metronidazole resistance in vitro. Parasitol Res. 2006;100(1):123–30.
31. Diamond LS. The establishment of various trichomonads of animals and man in axenic cultures. J Parasitol. 1957;43(4):488–90.
32. Mantovani A, Polentarutti N, Peri G, Martinotti G, Landolfo S. Cytotoxicity of human peripheral blood monocytes against Trichomonas vaginalis. Clin Exp Immunol. 1981;46(2):391–6.
33. Alderete JF, Garza GE. Specific nature of Trichomonas Vaginalis parasitism of host cell surfaces. Infect Immun. 1985;50(3):701–8.
34. Alderete JF. Epitopes within recombinant α-actinin protein is serodiagnostic target for Trichomonas Vaginalis sexually transmitted infections. Heliyon. 2017;3(1):e00237.
35. Alderete JF, Chan H. Point-of-Care Diagnostic for Trichomonas Vaginalis, the most Prevalent, non-viral sexually transmitted infection. Pathogens. 2023;12(1).
36. Alderete JF, Neace CJ. Identification, characterization, and synthesis of peptide epitopes and a recombinant six-epitope protein for Trichomonas vaginalis serodiagnosis. Immunotargets Ther. 2013;2:91–103.
37. Jesus JB, Vannier-Santos MA, Britto C, Godefroy P, Silva-Filho FC, Pinheiro AA, et al. Trichomonas vaginalis virulence against epithelial cells and morphological variability: the comparison between a well-established strain and a fresh isolate. Parasitol Res. 2004;93(5):369–77.
38. Krvavac S. Trichomoniasis and cystic fibrosis. Postgrad Med J. 1990;66(772):155–6.
39. Rein MF, Sullivan JA, Mandell GL. Trichomonacidal activity of human polymorphonuclear neutrophils: killing by disruption and fragmentation. J Infect Dis. 1980;142(4):575–85.
40. Mercer F, Ng SH, Brown TM, Boatman G, Johnson PJ. Neutrophils kill the parasite trichomonas vaginalis using trogocytosis. PLoS Biol. 2018;16(2):e2003885.
41. Trujillo EN, Flores BA, Romero IV, Moran JA, Leka A, Ramirez AD, et al. Complement receptor 3 is required for maximum in vitro trogocytic killing of the parasite trichomonas vaginalis by human neutrophil-like cells. Parasite Immunol. 2024;46(2):e13025.
42. Bhakta SB, Moran JA, Mercer F. Neutrophil interactions with the sexually transmitted parasite trichomonas vaginalis: implications for immunity and pathogenesis. Open Biol. 2020;10(9):200192.
43. Matlung HL, Babes L, Zhao XW, van Houdt M, Treffers LW, van Rees DJ, et al. Neutrophils kill antibody-opsonized Cancer cells by Trogoptosis. Cell Rep. 2018;23(13):3946–e596.
44. Bal MS, Singla LD, Kumar H, Vasudev A, Gupta K, Juyal PD. Pathological studies on experimental Trypanosoma Evansi infection in Swiss albino mice. J Parasit Dis. 2012;36(2):260–4.
45. Hersh SM. Pulmonary trichomoniasis and Trichomonas tenax. J Med Microbiol. 1985;20(1):1–10.
46. Hammond TL, Hankins GD, Snyder RR. Transvaginal-peritoneal migration of Trichomonas Vaginalis as a cause of ascites. A report of two cases. J Reprod Med. 1990;35(2):179–81.
47. Suriyanon V, Nelson KE. Choomsai na Ayudhya V. Trichomonas vaginalis in a perinephric abscess. A case report. Am J Trop Med Hyg. 1975;24(5):776–80.

Publisher's note

Springer Nature remains neutral with regard to jurisdictional claims in published maps and institutional affiliations.